Combined Diffusion and Perfusion MR Imaging as Biomarkers of Prognosis in Immunocompetent Patients with Primary Central Nervous System Lymphoma

F.E. Valles, C.L. Perez-Valles, S. Regalado, R.F. Barajas, J.L. Rubenstein, and S. Cha

ABSTRACT

BACKGROUND AND PURPOSE: ADC derived from DWI has been shown to correlate with PFS and OS in immunocompetent patients with PCNSL. The purpose of our study was to confirm the validity of ADC measurements as a prognostic biomarker and to determine whether rCBV measurements derived from DSC perfusion MR imaging provide prognostic information.

MATERIALS AND METHODS: Pretherapy baseline DWI and DSC perfusion MR imaging in 25 patients with PCNSL was analyzed before methotrexate-based induction chemotherapy. Contrast-enhancing tumor was segmented and coregistered with ADC and rCBV maps, and mean and minimum values were measured. Patients were separated into high or low ADC groups on the basis of previously published threshold values of $ADC_{min} < 384 \times 10^{-6}$ mm^2/s. High and low rCBV groups were defined on the basis of receiver operating curve analysis. High and low ADC and rCBV groups were analyzed independently and in combination. Multivariate Cox survival analysis was performed.

RESULTS: Patients with ADC_{min} values $< 384 \times 10^{-6}$ mm^2/s or $rCBV_{mean}$ values < 1.43 had worse PFS and OS. The patient cohort with combined low ADC_{min}–low $rCBV_{mean}$ had the worst prognosis. No other variables besides ADC and rCBV significantly affected survival.

CONCLUSIONS: Our study reinforces the validity of ADC values as a prognostic biomarker and provides the first evidence of low tumor rCBV as a novel risk factor for adverse prognosis in immunocompetent patients with PCNSL.

ABBREVIATIONS: CEL = contrast-enhancing lesion; DSC = dynamic susceptibility-weighted contrast-enhanced; min = minimum; OS = overall survival; PCNSL = primary central nervous system lymphoma; PFS = progression-free survival; rCBV = relative cerebral blood volume

PCNSL, an extra-nodal variant of non-Hodgkin lymphoma confined to the CNS,[1] is an aggressive primary brain cancer with rising incidence and variable response to therapy and clinical outcome.[2-4] Unlike systemic lymphomas, relatively little is known about the pathobiology of PCNSL.[5] Immune deficiency is the only established risk factor for developing PCNSL with uniformly devastating clinical outcome.[6] In immunocompetent individuals, however, the disease etiology remains unknown and prognosis can be highly variable.[7] Several markers of adverse prognosis have been suggested such as age older than 60 years, low performance scores, high lactate dehydrogenase level, high CSF protein level, enhancing lesions involving the brain stem,[8,9] and no initial response to steroids.[10] However, noninvasive biomarkers of prognosis and tumor biology that can be measured serially and quantitatively are needed to identify high-risk subgroups at initial diagnosis for formulation of a personalized therapeutic strategy, to assess response to therapy, and to detect tumor recurrence without delay.

Physiology-based MR imaging modalities, such as DWI and DSC perfusion MR imaging, are used clinically to characterize tumor biology beyond structural abnormalities.[11] A recently published report suggests a significant correlation between DWI-derived ADC values and clinical outcomes of immunocompetent patients with PCNSL treated with high-dose methotrexate. Specifically, pretherapeutic minimum ADC values $<384 \times 10^{-6}$ mm^2/s within enhancing tumor were predictive of shorter progression-free and overall survival.[12] Although there are no published data on DSC perfusion MR imaging and

Received December 12, 2011; accepted after revision March 13, 2012.

From the Departments of Radiology and Biomedical Imaging (F.E.V., C.L.P.-V., S.R., R.F.B., S.C.) and Medicine, Division of Hematology/Oncology (J.L.R.), University of California San Francisco School of Medicine, San Francisco, California.

This publication was supported by NIH/NCRR/OD UCSF-CTSI grant No. TL1RR024129. The study was funded in part by the Leukemia and Lymphoma Society, the UCSF Brain Tumor Specialized Programs of Research Excellence, and NIH R01CA1398301.

The contents of this article are solely the responsibility of the authors and do not necessarily represent the official views of the NIH.

Paper previously presented in part at: 49th Annual Meeting of the American Society of Neuroradiology, June 4–June 9, 2011; Seattle, Washington.

Please address correspondence to Soonmee Cha, MD, UCSF Department of Radiology, 350 Parnassus Ave, Suite 307, Room 307H, Box 0336, San Francisco, CA 94117; e-mail: soonmee.cha@ucsf.edu

Indicates open access to non-subscribers at www.ajnr.org

http://dx.doi.org/10.3174/ajnr.A3165

prognosis in patients with PCNSL, there are several studies that have demonstrated the value of rCBV as a predictor of grade and prognosis in gliomas.[13-16]

The purpose of our study was to confirm the validity of ADC measurement as a prognostic biomarker and to determine whether rCBV measurements derived from DSC perfusion MR imaging provide prognostic information.

MATERIALS AND METHODS

Patient Population

Twenty-five patients treated at our institution between June 2001 and July 2009 were selected for this retrospective study on the basis of the following criteria: histopathologic diagnosis of B-cell PCNSL as defined by the World Health Organization; negative immunodeficiency virus status; and absence of disease outside the CNS based on CT scans of the chest, abdomen, and pelvis. All patients had a pathologic diagnosis of large B-cell CNS lymphoma and received identical methotrexate-based induction chemotherapy treatment. Of 121 patients who met the inclusion criteria for this investigation, 25 had both diffusion and perfusion MR imaging available for analysis before their diagnostic biopsy. Of the 25, 15 were women and 10 were men. The average performance score at pretherapy baseline was 69.2 with a range of 50–100.

The induction chemotherapy (cycle = 28 days, 4 cycles) comprised a 3-drug regimen: methotrexate, 8 g/m^2, days 1 and 15; temozolomide, 150–200 mg/m^2/day, days 7–11; and rituximab, 375 mg/m^2, every week. In patients who achieved a complete response, defined as complete resolution of contrast-enhancing lesions on follow-up MR imaging, to induction therapy, 2–3 additional cycles of methotrexate (8 g/m^2) were administered every 14–21 days as consolidation therapy. Patients who achieved a partial response, defined as an interval decrease in the contrast-enhancing lesion, or who exhibited disease progression, defined by an increase in contrast-enhancing lesion volume or development of new enhancing lesions on follow-up MR imaging, were offered high-dose chemotherapy including methotrexate or whole-brain irradiation as salvage therapy. All patients with PCNSL included in this study underwent restaging with follow-up MR imaging within 5 cycles of methotrexate chemotherapy.[2] The clinical performance score, the Karnofsky Performance Score, was assessed at pretherapy baseline evaluation.

MR Imaging Protocol

The imaging protocols consisted of preoperative MR imaging performed on a 1.5T clinical scanner (Signa Horizon; GE Healthcare, Milwaukee, Wisconsin). The MR imaging protocol was as follows: 3-plane localizer, sagittal T1-weighted spin-echo (TR/TE, 600/17 ms), axial 3D T2-weighted fast spin-echo (TR/TE, 3000/102 ms), axial FLAIR (TR/TE/TI, 10,000/148/2200 ms), axial DWI (TR/TE, 10,000/99 ms; section thickness/intersection gap, 5/0 mm; matrix size, 256 × 256; FOV, 24 cm; 3 orthogonal diffusion gradient direction; b-values, 0 and 1000 s/mm^2) acquired in the transverse plane covering the whole brain, DSC perfusion MR imaging, contrast-enhanced 3D spoiled gradient-recalled T1-weighted imaging (TR/TE, 34/8 ms; section thickness/intersection gap, 1.5/0 mm), and axial T1-weighted postcontrast spin-echo imaging (TR/TE, 500/20 ms).

The standard DSC perfusion MR imaging protocol (TR/TE, 1250/54; flip angle 35°) at our institution was used to acquire a series of gradient-echo echo-planar images immediately before, during, and after a bolus injection of gadolinium diethylene triamine pentaacetic acid (Magnevist; Bayer Healthcare, Wayne, New Jersey). Eight axial 4-mm-thick sections were used to cover the entire tumor volume, as determined with T2-weighted FLAIR images. The first 10 echo-planar acquisitions were performed before gadolinium diethylene triamine pentaacetic acid (0.1 mmol/Kg body weight) was injected intravenously by using an MR imaging–compatible power injector (Spectris Solaris; MedRad, Indianola, Pennsylvania) at a rate of 4–5 mL/s through a 18- or 20-ga angiocatherer and followed immediately by a 20-mL continuous saline flush. A multisection image set was obtained every 1.25 seconds before, during, and after the first pass of contrast agent until images were obtained at 60 time points.

MR Image Processing

The contrast-enhanced 3D spoiled gradient-recalled images and raw diffusion data were transferred to a commercially available workstation, aligned to the same axial location, and processed by using FuncTool software and the Advantage workstation (GE Healthcare). ADC maps were calculated on a voxel-by-voxel basis from the diffusion imaging sets. ADC measurements of the contrast-enhancing tumor volume were measured. The average ADC_{min} values in units of 10^{-6} mm^2/s for all ROIs were calculated. The investigator responsible for production of the region of interest was blinded to pathologic and clinical outcome (F.E.V.). All ROIs were approved by an attending neuroradiologist certified by the American Board of Radiology with a Certificate of Added Qualification in neuroradiology (S.C.).

The raw data of T2*-weighted DSC perfusion MR images were transferred to the same workstation as mentioned above. rCBV maps were derived by using the methods published previously.[17] Contrast-enhanced 3D spoiled gradient-recalled images with ROIs of enhancing tumor were aligned with rCBV maps by using the aforementioned image-processing software. In addition, one 50-mm^2 region of interest was manually drawn around the enhancing region with the higher CBV for each transaxial section. A 50-mm^2 region of interest within the contralateral normal-appearing white matter for each transaxial section was used to standardize the CBV measurements ($rCBV_{mean}$ and $rCBV_{min}$).

Statistical Analysis

The ADC_{min} group was stratified into low ADC_{min} (< 384) and high ADC_{min} (≥ 384) subgroups. The $rCBV_{mean}$ group was stratified into low $rCBV_{mean}$ (<1.43) and high $rCBV_{mean}$ (≥ 1.43) subgroups by using a receiver operating characteristic analysis. Similar analysis for the $rCBV_{min}$ yielded a low $rCBV_{min}$ subgroup (<0.56) and a high $rCBV_{min}$ subgroup (≥ 0.56).

Using the Wilcoxon rank sum test, we performed multiple-comparison analysis among the 4 groups (high ADC/high rCBV, high ADC/low rCBV, low ADC/high rCBV, and low ADC/low rCBV). Univariate analyses were performed comparing patient age at diagnosis, CEL volume, edema volume, ADC values, and rCBV values.

Two clinical end points were measured in months: OS and

Patient demographics and imaging characteristics

Patient No.	Age (yr)/ Sex	$ADC_{min} \times 10^{12}$	ADC Group	CEL (vol · cm^3)	Edema (vol · cm^3)	$rCBV_{mean}$	$rCBV_{mean}$ Group	$rCBV_{min}$	$rCBV_{min}$ Group
1	80/M	520	High	11.37	108.63	1.02	Low	0.01	Low
2	60/M	618	High	6.26	29.37	1.43	Low	0.40	Low
3	70/F	575	High	12.62	96.00	1.38	Low	0.33	Low
4	58/M	133	Low	49.10	153.20	1.00	Low	0.50	Low
5	74/F	213	Low	43.40	99.30	1.42	Low	0.26	Low
6	59/F	594	High	20.04	72.43	1.17	Low	0.26	Low
7	53/F	236	Low	6.90	62.60	1.15	Low	0.25	Low
8	64/F	631	High	6.39	41.62	1.16	Low	0.52	Low
9	71/F	279	Low	28.89	152.69	1.01	Low	0.27	Low
10	58/F	660	High	18.80	193.90	1.17	Low	0.34	Low
11	76/M	640	High	5.00	26.10	2.82	High	0.18	Low
12	88/M	580	High	14.70	112.60	2.76	High	1.19	High
13	84/M	620	High	14.18	89.76	2.62	High	0.50	Low
14	57/F	528	High	13.90	30.50	1.61	High	0.89	High
15	64/M	260	Low	39.45	218.88	1.67	High	0.02	Low
16	64/F	718	High	11.94	50.49	4.39	High	1.19	High
17	87/F	586	High	4.06	91.71	2.37	High	0.55	Low
18	68/F	1010	High	8.40	19.60	1.80	High	1.16	High
19	74/M	684	High	16.86	130.90	1.79	High	0.22	Low
20	30/M	505	High	29.00	186.10	4.21	High	1.29	High
21	70/F	233	Low	22.60	102.20	1.90	High	0.02	Low
22	83/F	409	High	8.85	94.84	1.97	High	0.38	Low
23	68/M	562	High	22.60	115.20	1.60	High	0.95	High
24	60/F	737	High	3.06	45.38	1.50	High	0.34	Low
25	59/F	318	Low	17.48	56.36	1.72	High	0.59	High

PFS, defined as the time from initiation of therapy to death and to the first recurrence, respectively. A single covariate survival analysis was performed by using a logrank test. A Cox proportional hazards model was used for multivariable survival analysis. A P value $<.05$ was considered to indicate a significant difference between groups.

RESULTS

Anatomic Tumor Burden at Pretherapy Baseline Does Not Predict Clinical Outcome

The CEL volume varied from 5.0 to 39.45 cm^3 (mean, 17.43 ± 12.35 cm^3), and the peritumoral edema volume ranged from 19.6 to 218.88 cm^3 (95.21 ± 54.65 cm^3). Cox multivariate survival analysis showed that CEL volume, edema volume, age, and Karnofsky Performance Score did not influence PFS or OS ($P > .05$). The Table summarizes patient demographics and MR imaging variables at pretherapy baseline.

Lower Pretherapy Baseline ADC_{min} Measurements Predict Shorter Survival

Within the patient cohort, we identified a wide range (133–1010 × 10^{-6} mm^2/s) of intertumoral variability in pretherapy ADC_{min} values. Seven of the 25 patients included in this study had an $ADC_{min} < 384$ within enhancing regions and were assigned to the low ADC_{min} subgroup. The remaining 18 patients ($ADC_{min} \geq 384$) were designated as the high ADC_{min} subgroup. As shown in Fig 1, patients in the low ADC_{min} subgroup had a greatly increased risk of both progression ($P < .01$ logrank test, hazard ratio = 0.24; Fig 1*D*) and death ($P = 0.02$, hazard ratio = 0.29; Fig 1*A*) compared with the high ADC_{min} group. Mean PFS and mean OS were significantly shorter in the low ADC_{min} group versus the high ADC_{min} group ($P = .04$ and $P = .05$, respectively).

Lower Pretherapy Baseline $rCBV_{mean}$ and $rCBV_{min}$ Measurements Predict Adverse Outcome

Ten of the 25 patients in the study with $rCBV_{mean}$ values <1.43 were assigned to the low $rCBV_{mean}$ subgroup, and the remaining 15 patients with $rCBV_{mean} \geq 1.43$ were designated as the high $rCBV_{mean}$ subgroup. Patients in the low $rCBV_{mean}$ subgroup had increased risk for both rapid progression ($P = .03$ logrank test, hazard ratio = 0.28; Fig 1*E*) and death ($P = .03$ logrank test, hazard ratio = 0.30; Fig 1*B*).

Eighteen of the 25 patients had $rCBV_{min}$ values < 0.56 and were designated the low $rCBV_{min}$ subgroup, and the remaining 7 patients ($rCBV_{min} \geq 0.56$) were assigned to the high $rCBV_{min}$ subgroup. When patient outcome was stratified by $rCBV_{min}$, the low subgroup had increased risk for rapid progression ($P < .01$, logrank test; Fig *1F*) and death ($P = .01$, logrank test; Fig 1*C*).

Combined ADC-rCBV Groups Are Predictive of Outcomes in Which the Low ADC–low rCBV Group Has the Worst Prognosis

To evaluate the potential additive effects of ADC and rCBV stratification methods, we grouped patient cohorts by using a combined stratification method. Figure 2 illustrates survival difference among different combinations of the ADC-rCBV cohort, in which patients in the low ADC–low rCBV group had the greatest risk for both rapid disease progression ($P < .01$, logrank test) and death ($P < .01$, logrank test).

The PFS outcomes (Fig 2*C*, -*D*) were observed to cluster into nonbimodal cohorts, while the overall survival outcomes (Fig 2*A*, -*B*) were observed to cluster into bimodal cohorts for both categorization strategies.

When we compared the combined variables with each individual variable, the overall survival is better stratified into high and

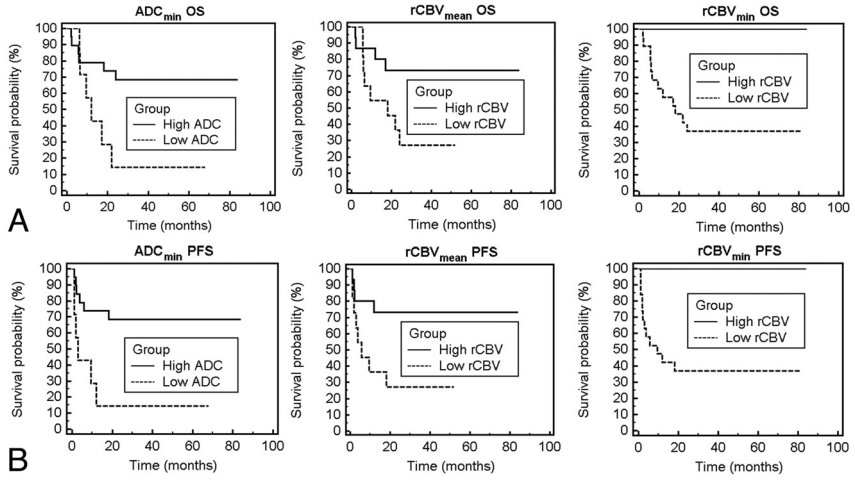

FIG 1. Overall survival and progression-free survival probability based on ADC or rCBV measurements. *A* and *D*, Patient outcome as a function of ADC_{min} stratification into low and high groups. Kaplan-Meier analysis (*A*) of OS for patients stratified into the low group ($ADC_{min} < 384$, dashed line) with a mean survival of 12.1 months versus those stratified into the high group ($ADC_{min} \geq 384$, solid line) with a mean survival time of 20.1 months ($P = .02$, logrank test). Kaplan-Meier plot (*D*) of PFS stratified into the same low group ($ADC_{min} < 384$, dashed line) with a mean progression time of 13.8 months versus those stratified into the high group ($ADC_{min} \geq 384$, solid line) with a mean progression time of 38.9 months ($P < .01$, logrank test). *B* and *E*, Patient outcome as a function of $rCBV_{mean}$ shows a statistically significant difference in OS and PFS between low ($rCBV_{mean} < 1.43$) and high ($rCBV_{mean} \geq 1.43$) groups ($P = .03$, logrank test for OS; $P = .03$, logrank test for PFS). *C* and *F*, Patient outcome as a function of $rCBV_{min}$ shows a statistically significant difference in OS and PFS between low ($rCBV_{min} < 0.56$) and high ($rCBV_{min} \geq 0.56$) groups ($P = .01$, logrank test for OS; $P < .01$, logrank test for PFS).

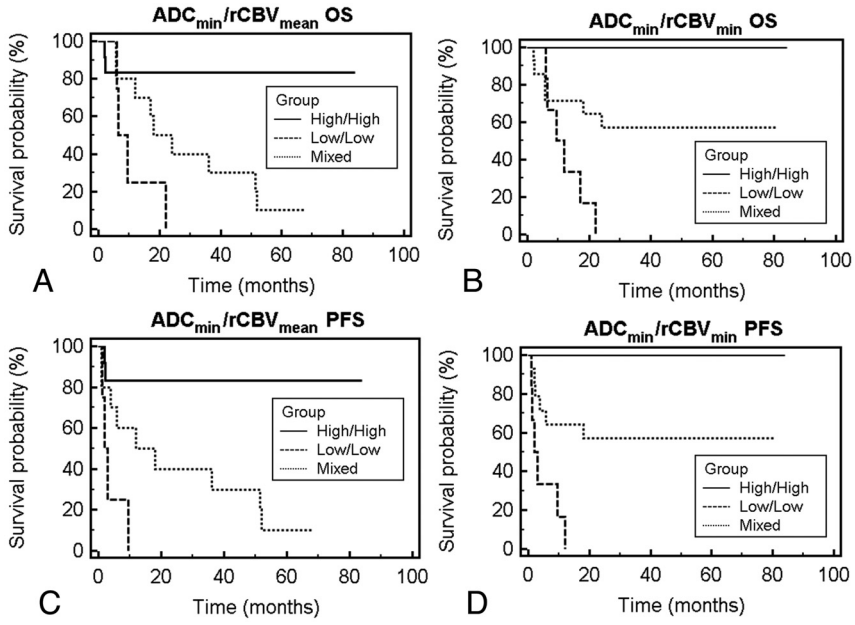

FIG 2. Overall survival and progression-free survival probability based on combined ADC and rCBV measurements. *A* and *C*, Patient outcome as a function of combined stratification by using ADC_{min} and $rCBV_{mean}$. Patients stratified into the low-low group ($ADC_{min} < 384$, $rCBV_{mean} < 1.43$; dashed line), high-high group ($ADC_{min} \geq 384$, $rCBV_{mean} \geq 1.43$; solid line), and mixed (low ADC_{min} and high $rCBV_{mean}$ or high ADC_{min} and low $rCBV_{mean}$; dotted line). Kaplan-Meier analysis (*A*) of OS shows decreased median survival for the low-low group of 7.9 months and a median survival of 36.0 months for the mixed group ($P < .01$, logrank test). Kaplan-Meier analysis (*C*) of PFS shows a median progression for the low-low group of 2.5 months and a median progression of 36 months for the mixed group ($P < .01$, logrank test). *C* and *D*, Patient outcome as a function of combined stratification by using ADC_{min} and $rCBV_{min}$: patients stratified into the low-low group ($ADC_{min} < 384$, $rCBV_{min} < 0.56$; dashed line), high-high group ($ADC_{min} \geq 384$, $rCBV_{min} \geq 0.56$; solid line), and mixed (low ADC_{min} and high $rCBV_{min}$ or high ADC_{min} and low $rCBV_{min}$; dotted line). Kaplan-Meier analysis shows statistically significant differences between groups in overall survival and progression ($P < .01$, logrank test for OS; $P < .01$, logrank test for PFS).

low survival groups by using both ADC and rCBV than by using only 1 individual variable as shown in Fig 3. The high ADC–high rCBV group and the high ADC group have statistically different survival rates ($P = .01$); similarly the low ADC–low rCBV group and the low rCBV group have different survival rates ($P = .03$).

DISCUSSION

Here, we confirm the validity of ADC measurement as a prognostic biomarker and present the first evidence of rCBV values as an additional imaging biomarker of clinical outcome in patients with PCNSL. In this study, we reproduced the previously reported finding of tumor ADC values derived from DWI as a powerful predictor of clinical outcomes in immunocompetent patients with PCNSL who are treated uniformly with methotrexate-based chemotherapy. We found that the lower the pretherapy baseline tumor ADC values, the shorter the PFS and OS in this group of patients with lymphoma. Both mean and minimum ADC values of tumor at pretherapy show a strong statistical correlation with clinical end points of PFS and OS. When the patients were separated into high-risk (low ADC) versus low-risk (high ADC) subgroups based on the previously published cutoff value of $ADC_{min} < 384 \times 10^{-6}$ mm^2/s, the difference in clinical outcomes between the 2 groups was highly significant, in that the low-risk group had a greater than 2-fold increase in OS and an almost 3-fold increase in PFS compared with the high-risk group.

The exact biologic or molecular correlate of ADC measurement in PCNSL remains unclear. Previous studies have shown significant inverse correlation between tumor cell attenuation and ADC values in PCNSL, suggesting ADC as a surrogate marker of tumor proliferation. Summarizing from numerous published reports on DWI of gliomas in which ADC values have been closely linked to tumor cell attenuation and nuclear-to-cytoplasmic ratio,[18-21] one can postulate that ADC values in PCNSL are imaging surrogates of tumor cell attenuation and that lower ADC values reflect higher cellular proliferation in PCNSL, hence correlating with adverse clinical outcome.

We found those patients with low tumor

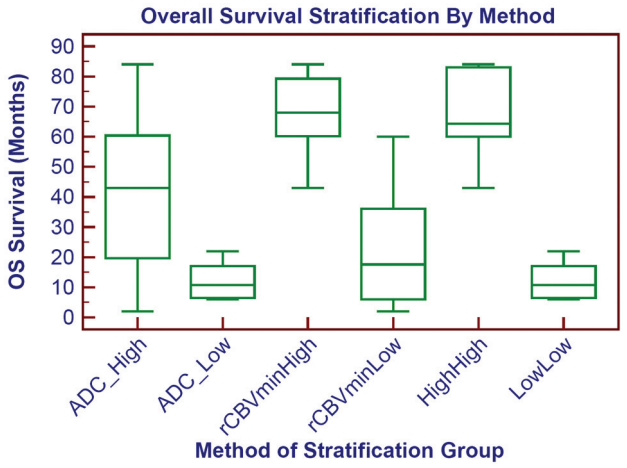

FIG 3. Prognostic survival groups based on individual or combined imaging variables. Overall survival stratification based on ADC_{min}, $rCBV_{min}$, or combined ADC_{min}–$rCBV_{min}$ is shown as a boxplot. The survival difference is most marked when comparing the combined low ADC_{min}–low $rCBV_{min}$ (low-low) group and the high ADC_{min}–high $rCBV_{min}$ (high-high). Similar results are obtained if $rCBV_{mean}$ is used instead of $rCBV_{min}$.

rCBV values (<1.43) at pretherapy baseline to have significantly shorter PFS and OS compared with the patients with high tumor rCBV values, similar to the ADC-based stratification. The biologic correlate of rCBV values in PCNSL remains conjectural, but one can postulate 2 possible explanations as to why low tumor rCBV values may be associated with adverse outcome in patients with PCNSL. First, rCBV values measure bulk vessel attenuation and thus reflect tumor angiogenesis. Second, rCBV values depend on patent vessels for delivery of intravenous gadolinium contrast agent. Therefore, low tumor rCBV values in PCNSL may signify a relative lack of tumor angiogenesis or a hypoxic microenvironment and decrease in patent vessels that are able to deliver intravenous methotrexate to the tumor bed. Our results are in agreement with the literature, in which PCNSL has been found to have hypoxic environments due to low perfusion[22] and these hypoxic environments lead to hypoxic tumors that are resistant to treatment.[23-25]

From further stratification based on a combination of ADC-rCBV values, we found the strongest imaging prediction of clinical outcomes in those patients with combined low tumor ADC and low rCBV values. The high ADC–high rCBV group had very low mortality (no patients died within 5 years), while the low ADC–low rCBV group had 100% mortality within 2 years (Fig 2*A*, -*B*). This new stratification suggests that the prognostic value of each imaging variable is additive and synergistic, in that the combination of both variables best predicted the worst prognostic subgroup of patients with PCNSL.

The results of our study have potentially high clinical impact in the treatment and management of patients with PCNSL. Noninvasive pretherapeutic imaging biomarkers that can accurately categorize patients into different risk groups of methotrexate-based chemotherapy could greatly facilitate clinical decision-making, allowing the initiation of individualized second-line salvage therapies, which may result in improved clinical outcome.[26-29] While ADC may signal a subtype of PCNSL that is more aggressive as demonstrated by cellularity,[12] our rCBV measure may help predict which tumors would be less treatable by chemotherapy due to lower perfusion.

Our study had several limitations. The results of our study may be influenced by its modest sample size and retrospective nature. Second, due to the paucity of available tumor-tissue samples, we were unable to correlate the rCBV measurements observed to histopathologic standards of tumor angiogenesis and hypoxia.

CONCLUSIONS

Our study further supports the important role of ADC measurement as a prognostic biomarker in immunocompetent patients with PCNSL in which the lower ADC measurement at pretherapy baseline indicates shorter overall survival. In addition, we present the first evidence of rCBV measurement as a potential prognostic biomarker in patients with PCNSL, in which lower value is associated with adverse prognosis. The predictive power of adverse outcome is even greater when risk stratification is based on combined low ADC and low rCBV values, suggesting the additive and complementary role of diffusion and perfusion MR imaging as prognostic biomarkers in patients with PCNSL.

Disclosures: Francisco Valles—*RELATED*: *Grant*: (Doris Duke Charitable Foundation Clinical Research Fellowships, *Comments*: The DDCF Clinical Research Fellowship program for medical students at UCSF is a 1-year mentored clinical research opportunity designed to span a broad range of research ranging from bench laboratory science to clinical and translational science, epidemiology, and outcomes research. We define "clinical and translational research" as research designed to address a question of clinical importance. The program is designed to be flexible and will be tailored to meet the needs of each student. James Rubenstein—*RELATED*: *Grant*: Dr Rubenstein is a Clinical Scholar of the Leukemia and Lymphoma Society and is a recipient of National Cancer Institute R01 CA139083–01A1.

REFERENCES

1. Deckert M, Engert A, Bruck W, et al. **Modern concepts in the biology, diagnosis, differential diagnosis and treatment of primary central nervous system lymphoma.** *Leukemia* 2011;25:1797–807
2. Olson JE, Janney CA, Rao RD, et al. **The continuing increase in the incidence of primary central nervous system non-Hodgkin lymphoma: a surveillance, epidemiology, and end results analysis.** *Cancer* 2002;95:1504–10
3. Eby NL, Grufferman S, Flannelly CM, et al. **Increasing incidence of primary brain lymphoma in the US.** *Cancer* 1988;62:2461–65
4. Schlegel U, Schmidt-Wolf IG, Deckert M. **Primary CNS lymphoma: Clinical presentation, pathological classification, molecular pathogenesis and treatment.** *J Neurol Sci* 2000;181:1–12
5. Hochberg FB, Hochberg E. **Primary CNS lymphoma.** *Nat Clin Pract Neurol* 2007;3:24–35
6. Wolf T, Brodt HR, Fichtlscherer S, et al. **Changing incidence and prognostic factors of survival in AIDS-related non-Hodgkin's lymphoma in the era of highly active antiretroviral therapy (HAART).** *Leuk Lymphoma* 2005;46:207–15
7. Bayraktar S, Bayraktar UD, Ramos JC, et al. **Primary CNS lymphoma in HIV positive and negative patients: comparison of clinical characteristics, outcome and prognostic factors.** *J Neurooncol* 2011;101:257–65
8. Abrey LE, Batchelor TT, Ferreri AJ, et al, for the International Primary CNS Lymphoma Collaborative Group. **Report on an international workshop to standardize baseline evaluation and response criteria for primary CNS lymphoma.** *J Clin Oncol* 2005;23:5034–43
9. Ferreri AJ, Blay JY, Reni M, et al. **Prognostic scoring system for primary CNS lymphomas: the international extranodal lymphoma study group experience.** *J Clin Oncol* 2003;21:266–72
10. Mathew BS, Carson KA, Grossman SA. **Initial response to glucocorticoids.** *Cancer* 2006;106:383–87
11. Cha S. **Update on brain tumor imaging: from anatomy to physiology.** *AJNR Am J Neuroradiol* 2006;27:475–87
12. Barajas RF Jr, Rubenstein JL, Chang JS, et al. **Diffusion-weighted MR imaging derived apparent diffusion coefficient is predictive of clin-**

ical outcome in primary central nervous system lymphoma. *AJNR Am J Neuroradiol* 2009;31:60–66
13. Hirai T, Murakami R, Nakamura H, et al. **Prognostic value of perfusion MR imaging of high-grade astrocytomas: Long-term follow-up study.** *AJNR Am J Neuroradiol* 2008;29:1505–10
14. Whitmore RG, Krejza J, Kapoor GS, et al. **Prediction of oligodendroglial tumor subtype and grade using perfusion weighted magnetic resonance imaging.** *J Neurosurg* 2007;107:600–09
15. Chaskis C, Stadnik T, Michotte A, et al. **Prognostic value of perfusion-weighted imaging in brain glioma: a prospective study.** *Acta Neurochir (Wien).* 2006;148:277–85, discussion 285
16. Caseiras GB, Chheang S, Babb J, et al. **Relative cerebral blood volume measurements of low-grade gliomas predict patient outcome in a multi-institution setting.** *Eur J Radiol* 2010;73:215–20
17. Cha S, Lupo JM, Chen MH, et al. **Differentiation of glioblastoma multiforme and single brain metastasis by peak height and percentage of signal intensity recovery derived from dynamic susceptibility-weighted contrast-enhanced perfusion MR imaging.** *AJNR Am J Neuroradiol* 2007;28:1078–84
18. Guo AC, Cummings TJ, Dash RC, et al. **Lymphomas and high-grade astrocytomas: comparison of water diffusibility and histologic characteristics.** *Radiology* 2002;224:177–83
19. Herneth AM, Guccione S, Bednarski M. **Apparent diffusion coefficient: a quantitative parameter for in vivo tumor characterization.** *Eur J Radiol* 2003;45:208–13
20. Khayal IS, Vandenberg SR, Smith KJ, et al. **MRI apparent diffusion coefficient reflects histopathologic subtype, axonal disruption, and tumor fraction in diffuse-type grade II gliomas.** *Neuro Oncol* 2011;13:1192–201
21. Sugahara T, Korogi Y, Kochi M, et al. **Usefulness of diffusion-weighted MRI with echo-planar technique in the evaluation of cellularity in gliomas.** *J Magn Reson Imaging* 1999;9:53–60
22. Kim JA, Kim SJ, Do IG, et al. **Hypoxia-associated protein expression in primary central nervous system diffuse large b-cell lymphoma: does it predict prognosis?** *Leuk Lymphoma* 2011;52:205–13
23. Amberger-Murphy V. **Hypoxia helps glioma to fight therapy.** *Curr Cancer Drug Targets* 2009;9:381–90
24. Yetkin FZ, Mendelsohn D. **Hypoxia imaging in brain tumors.** *Neuroimaging Clin N Am* 2002;12:537–52
25. Knisely JP, Rockwell S. **Importance of hypoxia in the biology and treatment of brain tumors.** *Neuroimaging Clin N Am* 2002;12:525–36
26. Rubenstein JL, Fridlyand J, Abrey L, et al. **Phase I study of intraventricular administration of rituximab in patients with recurrent CNS and intraocular lymphoma.** *J Clin Oncol* 2007;25:1350–56
27. Soussain C, Hoang-Xuan K, Taillandier L, et al. **Intensive chemotherapy followed by hematopoietic stem-cell rescue for refractory and recurrent primary CNS and intraocular lymphoma: Société Française de Greffe de Moëlle Osseuse-Thérapie Cellulaire.** *J Clin Oncol* 2008;26:2512–18
28. Matsumoto Y, Horiike S, Fujimoto Y, et al. **Effectiveness and limitation of gamma knife radiosurgery for relapsed central nervous system lymphoma: a retrospective analysis in one institution.** *Int J Hematol* 2007;85:333–37
29. Ryken TC, Meeks SL, Pennington EC, et al. **Initial clinical experience with frameless stereotactic radiosurgery: analysis of accuracy and feasibility.** *Int J Radiat Oncol Biol Phys* 2001;51:1152–58